Published in final edited form as:
Neurogastroenterol Motil. 2010 October ; 22(10): e292–e300. doi:10.1111/j.1365-2982.2010.01538.x.

Origin, propagation and regional characteristics of porcine gastric slow wave activity determined by high-resolution mapping

J. U. Egbuji[1,2], **G. O'Grady**[1,2], **P. Du**[1], **L. K. Cheng**[1], **W. J. E. P. Lammers**[1,3], **J. A. Windsor**[2], and **A. J. Pullan**[1,4,5]

[1]Auckland Bioengineering Institute, The University of Auckland, Auckland, New Zealand [2]Department of Surgery, The University of Auckland, Auckland, New Zealand [3]Department of Physiology, Faculty of Medicine and Health Sciences, UAE University, Al Ain, United Arab Emirates [4]Department of Engineering Science, The University of Auckland, Auckland, New Zealand [5]Department of Surgery, Vanderbilt University, Nashville, TN, USA

Abstract

Background—The pig is a popular model for gastric electrophysiology studies. However, its normal baseline gastric activity has not been well characterized. High-resolution (HR) mapping has recently enabled an accurate description of human and canine gastric slow wave activity, and was employed here to define porcine gastric slow wave activity.

Methods—Fasted pigs underwent HR mapping following anesthesia and laparotomy. Flexible printed-circuit-board arrays were used (160–192 electrodes; spacing 7.62 mm). Anterior and posterior surfaces were mapped simultaneously. Activation times, velocities, amplitudes and frequencies were calculated, and regional differences evaluated.

Key Results—Mean slow wave frequency was 3.22 ± 0.23 cpm. Slow waves propagated isotropically from the pacemaker site (greater curvature, mid-fundus). Pacemaker activity was of higher velocity (13.3 ± 1.0 mm s^{-1}) and greater amplitude (1.3 ± 0.2 mV) than distal fundal activity (9.0 ± 0.6 mm s^{-1}, 0.9 ± 0.1 mV; $P < 0.05$). Velocities and amplitudes were similar in the distal fundus, proximal corpus (8.4 ± 0.8 mm s^{-1}, 1.0 ± 0.1 mV), distal corpus (8.3 ± 0.8 mm s^{-1}, 0.9 ± 0.2 mV) and antrum (6.8 ± 0.6 mm s^{-1}, 1.1 ± 0.2 mV). Activity was continuous across the anterior and posterior gastric surfaces.

Conclusions & Inferences—This study has quantified normal porcine gastric slow wave activity at HR during anesthesia and laparotomy. The pacemaker region was associated with high-

Address for Correspondence. Dr John Egbuji, Auckland Bioengineering Institute, The University of Auckland, Private Bag 92019, Auckland 1142, New Zealand. Tel: +64 21 02 654 007; fax: +64 9 367 7157; j.egbuji@auckland.ac.nz.

DISCLOSURES

None of the authors have any professional, financial or personal conflicts of interest in relation to this work.

CONTRIBUTIONS

JUE, GOG, PD designed and performed the research, analyzed data and wrote the paper. LKC and WJEPL assisted with experiments, data analysis, revised the manuscript and provided expert advice. JAW and AJP supervised the research, revised the manuscript and provided expert advice.

amplitude, high-velocity slow wave activity compared to the activity in the rest of the stomach. The increase in distal antral slow wave velocity and amplitude previously described in canines and humans is not observed in the pig. Investigators should be aware of these inter-species differences.

Keywords

gastric electrical activity; pacemaker; pig; stomach

INTRODUCTION

Gastric motility is initiated and coordinated by an underlying omnipresent slow wave activity, that is generated by the interstitial cells of Cajal (ICCs).[1] Slow waves propagate through the ICC networks and conduct to adjacent smooth muscle layers, inducing contractions when co-regulatory conditions are met, such as after a meal.[2] Loss of ICC networks and altered slow wave activity have been implicated in the pathogenesis of functional gastric disorders, such as gastroparesis, a condition in which the stomach fails to empty normally in the absence of an obstruction.[3]

The pig is increasingly being used as an animal model for *in vivo* studies of gastric slow wave activity and motility,[4–6] mainly because the pig is a monogastric omnivore like man and because they are relatively easy to source. However, very few studies have focused on describing the normal gastric slow wave activity of the pig, including the potential for regional variations in activity.[7] The availability of improved baseline data would be highly valuable to inform and facilitate future experimental studies using porcine models.

High-resolution (HR) slow wave mapping has been a significant recent advance for evaluating *in vivo* gastrointestinal (GI) slow wave activity. This technique involves the placement of spatially dense arrays of many electrodes over a defined area of tissue, with simultaneous recording from all sites, to accurately define the origin and sequence of slow wave propagation occurring in the target area.[8] HR mapping has recently been applied to define the propagation patterns of slow wave activity in the human and canine stomachs,[9,10] thereby revealing several new features that were not apparent in earlier sparse-electrode studies, including detailed representations of regional variations in slow wave activity.

The few previous studies of porcine gastric slow wave activity have relied on sparse-electrode techniques.[7,11] The aim of the current study was to employ modern HR mapping methods to accurately and comprehensively establish the baseline characteristics of slow wave activity in the porcine stomach. In addition, this study aimed to simultaneously map the slow wave propagation occurring over both the anterior and posterior gastric serosal surfaces, which has not been performed previously at HR. Comparisons were also made of gastric slow wave activity in the pig, human[10] and canine,[9] with a focus on the relative benefits and disadvantages of the porcine model for *in vivo* gastric slow wave investigations.

MATERIALS AND METHODS

Animal preparation

All experiments were performed *in vivo*. Ethical approval was obtained from The University of Auckland Animal Ethics Committee and the International Guiding Principles for Biomedical Research Involving Animals were followed. Sixteen white cross-breed weaner pigs were employed, of either sex and of mean weight 36.7 ± 0.5 kg. The pigs were fasted then subjected to general anesthesia that was induced with Zoletil (Tiletamine HCl 50 mg mL^{-1} and Zolazepam HCl 50 mg mL^{-1}), and maintained with Isoflurane (2.5–5% with an oxygen flow of 400 mL within a closed circuit anesthetic system). A possible alternative regimen of remifentanil/propofol has been found to be associated with pyloric spasm in pigs and therefore was not considered.[6]

A femoral artery was cannulated and vital signs were continuously monitored including heart rate and blood pressure. Rectal and intra-abdominal temperatures were also monitored, and these were kept in the normal physiological range (38.5–39.5 °C) by continuous use of a heating pad and the additional use of a heat lamp when necessary. A midline or bilateral subcostal laparotomy was performed depending on the gastric region of experimental interest, the latter incision being more suitable for investigations of the proximal stomach. At the conclusion of the experiments, the animals were euthanized with a bolus injection of 50 mL of magnesium sulfate while still under anesthesia.

Recording methods

High-resolution mapping was performed using flexible printed-circuit-board (PCB) multi-electrode arrays, which have been validated for this purpose.[8] Each PCB contained 32 individual electrodes arranged in a 4 × configuration, with an interelectrode distance of 7.62 mm (Fig. 1A). Between four and six PCBs were joined together in parallel alignment, with their noncontact surfaces secured together with adhesive tape, to map large areas of tissue simultaneously (128–192 electrodes total; mapped surface area 61–96 cm^2).

The abdominal walls were retracted, and the assembled PCBs were gently positioned over the serosal region of interest with minimal handling of the viscera. The array was then moved in a sequential manner over the stomach to consecutively map a large portion of the organ of each subject. After each positioning of the array, the PCBs were covered with warm (39 °C) saline-soaked gauze packs to secure them in place, and the wound edges were approximated, before the incision site was covered with warm wet packing to limit drying and cooling of the abdominal cavity. A 5 min period of stabilization was allowed prior to each recording.

Gastric regions and anatomical registration

The locations of the gastric fundus, corpus and antrum were defined for each subject with measurements from fixed anatomical landmarks (Fig. 1B). The fundus was defined as the region of the stomach proximal to the fundal line, a horizontal line drawn from the upper border of the gastro-esophageal junction (GEJ) to the greater curvature. The porcine GEJ is located at approximately the mid-point of the lesser curvature, meaning that a large portion

of the porcine stomach consists of fundus (Fig. 1B). The corpus and antrum were demarcated by a 45° line drawn from the incisura (a notch along the lesser curvature approximately midway between the GEJ and the pylorus) to the greater curvature. In addition, two specialized adaptations are present in the porcine stomach: (i) the gastric diverticulum, a distensible pouch surmounting the medial fundus; and (ii) the torus pyloricus, a fleshy protuberance accentuating the distal antrum and pylorus.[12]

At the beginning of each experiment, small sutures were placed in the omental fat adjacent to the above key anatomical landmarks, to ensure that the electrode arrays were consistently registered within each experimental animal. Diagrams and photographs were then obtained for each recording to document the array locations. At the conclusion of the experiments and before euthanasia, measurements of each subject's stomach were taken between the same landmark points, to permit accurate anatomical comparisons between all of the experimental animals.

In five animals, simultaneous mapping of the anterior and posterior serosal surfaces was undertaken. This was enabled by the flexibility of the PCBs, which allows them to conform to the shape of the greater curvature maintaining continuous serosal contact, except at the site of the gastroepiploic artery, which sits on the greater curvature. The porcine gastroepiploic artery leaves the stomach at the distal fundus. The tenuous greater omentum of the pig was divided to allow these experiments, and these recordings were performed in the final stage of the experiments.

Signal acquisition and processing

All recordings were acquired at a sampling frequency of 512 Hz using the ActiveTwo System (Biosemi, Amsterdam, Netherlands). The custom acquisition software was written in LabView v8.2 (National Instruments, Austin, TX, USA). The ActiveTwo System employs two reference electrodes termed the 'common mode sense' (CMS) and the 'right leg drive' (DRL) to form a feedback loop instead of a standard ground electrode. The CMS electrode was placed on the left lower abdomen, and the DRL electrode on the right hindquarter thigh. The slow wave recordings are referenced to the potential of the CMS electrode. Each recording array was connected via a 1.5 m 68-way ribbon cable to the ActiveTwo System, which was in turn connected to a Dell M1450 notebook computer via a fiber-optic cable.

After the recordings, slow wave activity was filtered with a second order Bessel low pass filter (2 Hz). Slow wave activity was quantified following each experiment by activation time (AT) mapping and calculation of regional velocities, amplitudes and frequencies. The slow wave AT were manually identified at the point of maximum negative slope of each event using SmoothMap v3.02[13] and activation maps were generated in MATLAB v.2006b (The Mathworks, Natick, MA, USA) (Fig. 1). Propagation velocities were calculated in SmoothMap, and plotted using a validated quadratic fitting method (MATLAB) that graphically represents the velocity at each electrode as a vector of size and length relative to the highest velocity vector in the array (Fig. 1F).[5,14] Amplitudes were calculated in SmoothMap as the difference between the maximum and the minimum voltage during a slow wave event (Fig. 1D). Frequency was determined from five separate electrodes by measuring and averaging the cycle-to-cycle interval of 15–30 successive slow wave cycles.

Dysrhythmic events sometimes occurred during the experiments, however, only normal slow wave activity was analyzed in the present study. Sets of 8–16 adjacent electrograms were examined at each slow wave cycle in every recording, and abnormal activity was defined and excluded as follows: (i) cycle-to-cycle variations in propagation direction and pattern[15]; and (ii) instances of regular or irregular brady- or tachygastria, defined as ≤2 and ≥4.5 cycles per minute (cpm) respectively.

Statistical analysis

Average regional amplitudes, velocities and frequencies were calculated (means ± SEM) for the fundus, corpus and antrum, as well as the pacemaker region, which was defined as the region activated within a 2 s period from the earliest AT.[9,10] A total of six regions were identified for the statistical analyses: the pacemaker area, proximal fundus, distal fundus, proximal corpus, distal corpus and antrum. The proximal fundus was defined as the area proximal to the pacemaker region, and the distal fundus as the area distal to the pacemaker region. The corpus was divided into proximal and distal halves. Population data was analyzed with one-way ANOVA tests, and if deemed significant ($P < 0.05$), further analysis using a Tukey post hoc test was employed to determine where the significant variation lay. Confidence intervals (CIs) of 95% are presented where appropriate.

RESULTS

A total of 97 separate recordings were made from the anterior and posterior gastric serosa of the 16 pigs, totalling 867 min (average duration of 8.9 ± 0.4 min per recording). In two of the experimental animals, only dysrhythmic activity was recorded, hence recordings from these two subjects were entirely excluded from further analysis. In total, fourteen segments of data (129 min; 15% of the signals recorded) were excluded from further analysis because they demonstrated dysrhythmic activities according to the specified criteria.

For the remaining recordings, the overall mean slow wave frequency was 3.22 ± 0.23 cpm, and there was no difference in frequency between any adjacent gastric regions ($P = 0.45$), indicating consistent entrainment and coupling of slow waves throughout the stomach.

Pacemaker and fundal activity

Fig. 2 displays representative electrograms, activation maps, and velocity field maps of slow wave activity in the pacemaker and fundal regions, as recorded in two animals. The pacemaker site (earliest recorded slow wave event) was localized in five pigs to the gastric mid-fundus at the greater curvature (Fig. 2). In the remaining subjects, this region was not mapped (n = 5), or the recording was of insufficient quality to define the site (n = 3). The pacemaker site was measured with further accuracy in four pigs, and was found to lie at approximately two-fifths of the distance from the fundal line to the apex of the fundus (i.e., median of 79 mm proximal to the fundal line (range 65–86 mm), with the median distance from fundal line to apex being 197 mm).

In all cases, slow waves propagated concentrically outward from the pacemaker region into an adjacent area of the fundus. However, the whole fundus was not activated, with the slow waves only propagating in the retrograde direction (toward the apex of the fundus) for a

mean distance of 33 ± 6 mm (n = 5) before terminating. Of the fundal regions that were activated, there was no difference in activity between the proximal and distal regions either in terms of velocity [8.1 ± 0.5 vs 9.0 ± 0.6 mm s^{-1}; mean difference = −0.9 mm s^{-1} (CI: −3.7, 1.9)] or amplitude [0.8 ± 0.1 vs 0.9 ± 0.1 mV; mean difference = 0.0 mV (CI: −0.04, 0.03)].

The velocity of the activity in the pacemaker region (13.3 ± 1.0 mm s^{-1}) was greater than that of the adjacent proximal fundus (8.1 ± 0.5 mm s^{-1}), [mean difference 5.2 mm s^{-1}, (CI: 2.0, 8.4); $P < 0.001$]; and distal fundus (9.0 ± 0.6 mm s^{-1}), [mean difference 4.3 mm s^{-1} (CI: 1.2, 7.4); $P < 0.01$]; (n = 5). In addition, the amplitude of slow waves in the pacemaker region (1.2 ± 0.2 mV) was higher than the amplitude of the activity in the adjacent proximal fundus (0.8 ± 0.1 mV), [mean difference 0.06 mV (CI: 0.01, 0.10); $P < 0.05$]; and distal fundus (0.9 ± 0.1 mV), [mean difference 0.05 mV (CI: 0.01, 0.10); $P < 0.05$]; (n = 5).

Slow wave velocity was found to be isotropic within the pacemaker area, with no significant difference found between the magnitude of the longitudinal (8.5 ± 0.5 mm s^{-1}) and circumferential (8.9 ± 0.9 mm s^{-1}) components of the velocity vectors ($P = 0.68$).

The amplitudes and velocities for the six stomach regions are summarized in Table 1.

Corpus and antrum activity

Activity propagated continuously from fundus to corpus (Figs 3 and 4). Distal to the fundus, the electrical activation occurred as a circumferential band propagating in the aboral direction (n = 14; Fig. 4). There was no significant difference in slow wave velocity between the proximal corpus (8.4 ± 0.8 mm s^{-1}) and distal corpus (8.3 ± 0.8 mm s^{-1}), [mean difference = 0.1 mm s^{-1} (CI: −2.9, 3.3)]; or between the distal corpus and the antrum (6.8 ± 0.6 mm s^{-1}) [mean difference = 1.5 mm s^{-1} (CI: −2.2, 5.2)]. Similarly, there was no difference in slow wave amplitudes between the proximal corpus (1.0 ± 0.1 mV) and distal corpus (0.9 ± 0.2 mV), [mean difference = 0.01 mV (CI: −0.03, 0.06)]; or between the distal corpus and the antrum (1.1 ± 0.2 mV), [mean difference 0.01 mV (CI: −0.06, 0.04)] (Table 1).

Areas of electrical quiescence

Antral slow waves were not recorded from the region of the torus pyloricus, and therefore slow waves did not propagate as far as the pyloric junction or duodenum. No slow waves were recorded from the cardia, the medial or superior fundus, fundal diverticulum, or from any region adjacent to the lesser curvature (Figs 5 and 6).

DISCUSSION

This study provides the first HR description of the normal pattern of slow wave propagation in the porcine stomach (Fig. 6). Recent technical advances in the hardware and software for HR slow wave mapping have been employed to present a substantially more detailed and comprehensive analysis than was possible with previous low-resolution (sparse electrode) approaches.[7] This study presents valuable baseline data, and offers the opportunity to

compare the porcine gastric conduction system with that recently determined at HR in the human[10] and in the dog.[9]

A number of recent studies have employed pigs for gastric slow wave investigations, including for the validation of new electrophysiology devices,[8,16] magnetometry measurements of gastric uncoupling,[4] gastric pacing and stimulation,[5,17] and motility studies.[6] Although dogs have traditionally been the large-animal model of choice for *in vivo* investigations of GI slow wave activity,[9,18,19] advantages for the increased use of pigs include the ease of accessing them through livestock farms, and reduced sourcing costs compared to dogs. Pigs are a theoretically suitable research model because, like humans, they are monogastric omnivores with a broadly comparable upper GI anatomy.

The results of this study confirm and expand what has recently been described in the human[10] and the canine stomach.[9] Importantly, regional variations in gastric slow wave activity are less marked in the pig than they are in the canine and the human. Most significantly, the marked transition in slow wave amplitude and velocity seen in the human antrum (2 times higher amplitude and 2 times greater velocity compared to human corpus)[10] and the canine antrum (2.2 times higher amplitude and 3 times higher velocity compared to the corpus),[9] was not observed in the pig. After the initial high-amplitude, high-velocity activity at the pacemaker site, porcine gastric slow wave propagation was found to be uniform throughout the remainder of the stomach whereas this was not the case in humans[10] and canines.[20]

Porcine gastric anatomy also demonstrates important differences from the gastric anatomy of either man or the dog, which appear more grossly similar. The porcine esophagus enters the stomach at the mid-lesser curvature, meaning the cardia is more distal and the anatomical fundal area is larger. No slow waves were detected at the site of the two anatomical specializations of the porcine stomach, the torus pyloricus (a muscular thickening of the distal antrum/pylorus) and the gastric diverticulum (a pouch surmounting the fundus). The stomach tissue adjacent to the lesser curvature was also found to be electrically quiescent. Previously, a histological examination of the mouse lesser curvature by Hirst *et al.*[21] revealed that the population of ICC-MY was highest along the greater curvature and was either sparse or absent along the lesser curvature. Similarly, Sarna *et al.*, years earlier had shown that slow waves were not usually recorded near the lesser curvature of the corpus in the fasted dog, but that the administration of acetylcholine could induce them.[22] More recently a study of rat gastric motility reported that contractions induced by a viscous perfusate were initially localized to the greater curvature, however, when more perfusate was added, the contractions gained in amplitude and extended to also involve the lesser curvature from a point just below the GEJ.[23] Therefore, it is possible that tissue areas close to the lesser curvature show quiescence in the fasted state, but may be recruited to entrained slow wave activity in a stimulated state, such as following a meal.

Slow wave velocity throughout the porcine stomach (~8 mm s^{-1}) is found to be higher than that of the human corpus (~3 mm s^{-1}) and canine corpus (~5 mm s^{-1}), being closer to the velocity of the activity of the human antrum (~6 mm s^{-1}).[9,10] Recent HR stomach mapping studies have shown that multiple slow wave fronts propagate simultaneously in the

longitudinal axis of the canine and human stomachs, at a separation that is dependent on the velocity and period of the slow waves.[9,10] The existence of multiple propagating wavefronts is of interest to investigators of electrogastrography and magnetogastrography, because the signals measured from the body surface represent a summation of multiple waves and cannot be directly related back to the specific individual events occurring in the stomach.[24,25] With a period of ~19 s, and a velocity of ~8 mm s^{-1}, the average spacing of slow waves in the porcine stomach is estimated from this study to be ~150 mm. Therefore, 1–2 slow waves will propagate simultaneously in the pig stomach compared to the multiple wavefronts propagating in the human stomach, where the average wavefront spacing in the corpus is ~60 mm.[10]

The findings of this study are comparable to a previous sparse-electrode study of conscious miniature Pitman-Moore pig stomachs (10–12 kg animals), by Roze *et al.*[7] The slow wave frequency in the miniature pigs was determined at 4.10 ± 0.04 cpm, compared to 3.22 ± 0.23 cpm in this study but their variations were quite large, ranging from 3.78 to 4.66 cpm. The different porcine slow wave frequency in that study may be attributable to breed differences. The propagation velocities in the miniature pig stomach was found to range from 5.8 ± 0.3 to 7.8 ± 0.3 mm s^{-1}, similar to the range of velocities in the fundus, corpus and antrum in this study. The presence and characteristics of the pacemaker region were missed in the previous sparse-electrode porcine study, as they were in previous canine and human sparse-electrode studies, due to the limitations of the low-resolution approach.[9,10]

For the first time, simultaneous recordings of the anterior and posterior gastric walls were performed and at high resolution. This was made possible by the flexibility of the PCB arrays,[8] and by the relatively rotated position of the porcine stomach compared to the canine and human, whereby the greater curvature is positioned ventrally, and the lesser curvature dorsally. The slow wave activity is found to propagate simultaneously and synchronously down both gastric surfaces, which in the contracting stomach, would give rise to a circumferential band of contraction that is witnessed during imaging.[26]

Like the few other HR mapping studies to date, the experiments here were performed in the fasted state under general anesthesia. In a recent HR study of human gastric slow wave activity in the anesthetized state, the overall description of slow wave propagation dynamics was in good agreement with the available data from imaging studies.[10] However, around 15% of the recordings in the current study were excluded because they demonstrated dysrhythmic activities. The cause of these dysrhythmias is unknown; however, the effects of anesthesia, the neurohormonal stress of laparotomy, and/or prostaglandin release induced by gastric handling could potentially have contributed.[27] Previous studies have also documented dysrhythmias arising in the context of anesthesia, surgery and visceral handing,[15,28] and we have also encountered sporadic dysrhythmias in the porcine stomach during attempts at gastric pacing.[5]

Propagating spike activity has previously been observed during HR mapping of the distal canine antrum,[9] however, it was not observed in this study. We have routinely recorded intestinal spike activity with this same system in other contexts (T. Angeli, W. Qiao, J. U. Egbuji, G. O'Grady, P. Du, L. Cheng, W. J. E. P. Lammers, J. A. Windsor, A. J. Pullan,

unpublished data), so we do not believe that the absence of spike recordings was a technical problem. Roze *et al*. described the variable presence of spike potentials in the distal stomach of conscious fasted miniature pigs *in vivo*, and described them to be three times more common after a meal.[7] The significance of spike activity in the porcine study would be better evaluated in the awake fed state, but it is not possible to perform this research at high resolution with current technology.

The findings of this study will also serve to inform further refinements of computational models of porcine gastric slow wave activity, which have the potential to improve research efficiency while reducing the animal burden and associated costs, compared to using purely experimental animal models.[29] Porcine gastric HR mapping has been recognized as a convenient method of informing and validating multiscale mathematical GI models,[30] and the results of the present study will be a valuable foundation for future work in this direction.

In summary, this study provides a detailed understanding of the origin and propagation of slow wave activity in the porcine stomach following anesthesia and laparotomy. The data presented will provide a useful baseline for investigators employing porcine models for slow wave investigations in future. There are significant differences in porcine activity compared to canine and human activity and further work is required to elucidate their underlying mechanisms and their impact on gastric motility.

Acknowledgments

We thank Linley Nisbet for her excellent technical assistance.

GRANTS

This work is supported by grants from the New Zealand Health Research Council, the NIH (R01 DK64775), the New Zealand Society of Gastroenterology/Ferring Pharmaceuticals Research Fellowship, The American Neurogastroenterology & Motility Society and the Auckland Medical Research Foundation.

REFERENCES

1. Sanders KM, Koh SD, Ward SM. Interstitial Cells of Cajal as pacemakers in the gastrointestinal tract. Annu Rev Physiol. 2006; 68:307–343. [PubMed: 16460275]
2. Huizinga JD, Lammers WJEP. Gut peristalsis is governed by a multitude of cooperating mechanisms. Am J Physiol Gastrointest Liver Physiol. 2009; 296:G1–G8. [PubMed: 18988693]
3. Farrugia G. Interstitial cells of Cajal in health and disease. Neurogastroenterol Motil. 2008; 20:54–63. [PubMed: 18402642]
4. Bradshaw LA, Irimia A, Sims JA, Richards WO. Biomagnetic signatures of uncoupled gastric musculature. Neurogastroenterol Motil. 2009; 21:778–e750. [PubMed: 19222760]
5. O'Grady G, Du P, Lammers WJ, Egbuji JU, Mithraratne P, Chen JD, Cheng LK, Windsor JA, Pullan AJ. High-resolution entrainment mapping of gastric pacing: a new analytical tool. Am J Physiol Gastrointest Liver Physiol. 2010 Feb; 298(2):G314–G321. [PubMed: 19926815]
6. Schnoor J, Bartz S, Klosterhalfen B, Kuepper W, Rossaint R, Unger JK. A long-term porcine model for measurement of gastrointestinal motility. Lab Anim. 2003; 37:145–154. [PubMed: 12689426]
7. Roze C, Couturier D, Debray C. Patterns of gastric electrical and motor activity in miniature pigs. Can J Physiol Pharmacol. 1976; 54:764–773. [PubMed: 1033025]

8. Du P, O'Grady G, Egbuji JU, et al. High-resolution mapping of in vivo gastrointestinal slow wave activity using flexible printed circuit board electrodes: methodology and validation. Ann Biomed Eng. 2009; 37:839–846. [PubMed: 19224368]
9. Lammers WJEP, Ver Donck L, Stephen B, Smets D, Schuurkes JAJ. Origin and propagation of the slow wave in the canine stomach: the outlines of a gastric conduction system. Am J Physiol Gastrointest Liver Physiol. 2009; 296:G1200–G1210. [PubMed: 19359425]
10. O'Grady G, Du P, Cheng LK, Egbuji JU, Lammers WJ, Windsor JA, Pullan AJ. Origin and propagation of human gastric slow-wave activity defined by high-resolution mapping. Am J Physiol Gastrointest Liver Physiol. 2010 Sep; 299(3):G585–G592. [PubMed: 20595620]
11. Wechsung E, Houvenaghel A. Effect of CCK-8 on myoelectrical activity of the gastrointestinal tract in the conscious miniature pig. Peptides. 1995; 16:1429–1432. [PubMed: 8745054]
12. Koenig, HE.; Liebich, HG. Veterinary Anatomy of Domestic Mammals. Textbook and Colour Atlas. Stuttgart: Schattauer; 2004.
13. Lammers, WJEP. SmoothMap. Version 3.02. 302 ed.. Wim Lammers: Al Ain, United Arab Emirates; 2008. Available at: http://www.smoothmap.org
14. Du P, Qiao W, O'Grady G, Egbuji JU, Lammers W, Cheng LK, Pullan AJ. Automated detection of gastric slow wave events and estimation of propagation velocity vector fields from serosal high-resolution mapping. Conf Proc IEEE Eng Med Biol Soc. 2009; 2009:2527–2530. [PubMed: 19964973]
15. Lammers WJEP, Ver Donck L, Stephen B, Smets D, Schuurkes JAJ. Focal activities and re-entrant propagations as mechanisms of gastric tachyarrhythmias. Gastroenterology. 2008; 135:1601–1611. [PubMed: 18713627]
16. O'Grady G, Du P, Egbuji JU, et al. A novel laparoscopic device for measuring gastrointestinal slow-wave activity. Surg Endosc. 2009; 23:2842–2848. [PubMed: 19466491]
17. Stecco KA, Snape JWJ. The use of a gastric pacing system with data telemetry to develop a chronic pacing non anesthetized porcine model. Gastroenterology. 2003; 124:A675–A675.
18. Kelly KA, Code CF. Canine gastric pacemaker. Am J Physiol. 1971; 220:112–118. [PubMed: 5538644]
19. Weber J Jr, Koatsu S. Pacemaker localization and electrical conduction patterns in the canine stomach. Gastroenterology. 1970; 59:717–726. [PubMed: 5475131]
20. Kelly KA, Code CF, Elveback LR. Patterns of canine gastric electrical activity. Am J Physiol. 1969; 217:461–470. [PubMed: 5812075]
21. Hirst GD, Beckett EA, Sanders KM, Ward SM. Regional variation in contribution of myenteric and intramuscular interstitial cells of Cajal to generation of slow waves in mouse gastric antrum. J Physiol. 2002; 540:1003–1012. [PubMed: 11986385]
22. Sarna SK, Daniel EE, Kingma YJ. Premature control potentials in the dog stomach and in the gastric computer model. Am J Physiol. 1972; 222:1518–1523. [PubMed: 5030211]
23. Lentle RG, Janssen PW, Goh K, Chambers P, Hulls C. Quantification of the effects of the volume and viscosity of gastric contents on antral and fundic activity in the rat stomach maintained ex vivo. Dig Dis Sci. 2010 Dec; 55(12):3349–3360. [PubMed: 20198425]
24. Verhagen MAMT, Van Schelven LJ, Samsom M, Smout AJPM. Pitfalls in the analysis of electrogastrographic recordings. Gastroenterology. 1999; 117:453–460. [PubMed: 10419928]
25. Kim J, Bradshaw L, Pullan A, Cheng L. Characterization of gastric electrical activity using magnetic field measurements: a simulation study. Ann Biomed Eng. 2010; 38:177–186. [PubMed: 19774463]
26. Pal A, Brasseur JG, Abrahamsson B. A stomach road or 'Magenstrasse' for gastric emptying. J Biomech. 2007; 40:1202–1210. [PubMed: 16934271]
27. Forrest AS, Hennig GW, Jokela-Willis S, Park CD, Sanders KM. Prostaglandin regulation of gastric slow waves and peristalsis. Am J Physiol Gastrointest Liver Physiol. 2009; 296:G1180–G1190. [PubMed: 19359421]
28. Hotokezaka M, Mentis EP, Patel SP, Combs MJ, Teates CD, Schirmer BD. Recovery of gastrointestinal tract motility and myoelectric activity change after abdominal surgery. Arch Surg. 1997; 132:410–417. [PubMed: 9108763]

29. Cheng LK, O'Grady G, Du P, Egbuji JU, Windsor JA, Pullan AJ. Gastrointestinal system. Wiley Interdiscip Rev Syst Biol Med. 2010 Jan-Feb;2(1):65–79. [PubMed: 20836011]

30. Du P, O'Grady G, Windsor JA, Cheng LK, Pullan AJ. A tissue framework for simulating the effects of gastric electrical stimulation and in vivo validation. IEEE Trans Biomed Eng. 2009; 56:2755–2761. [PubMed: 19643697]

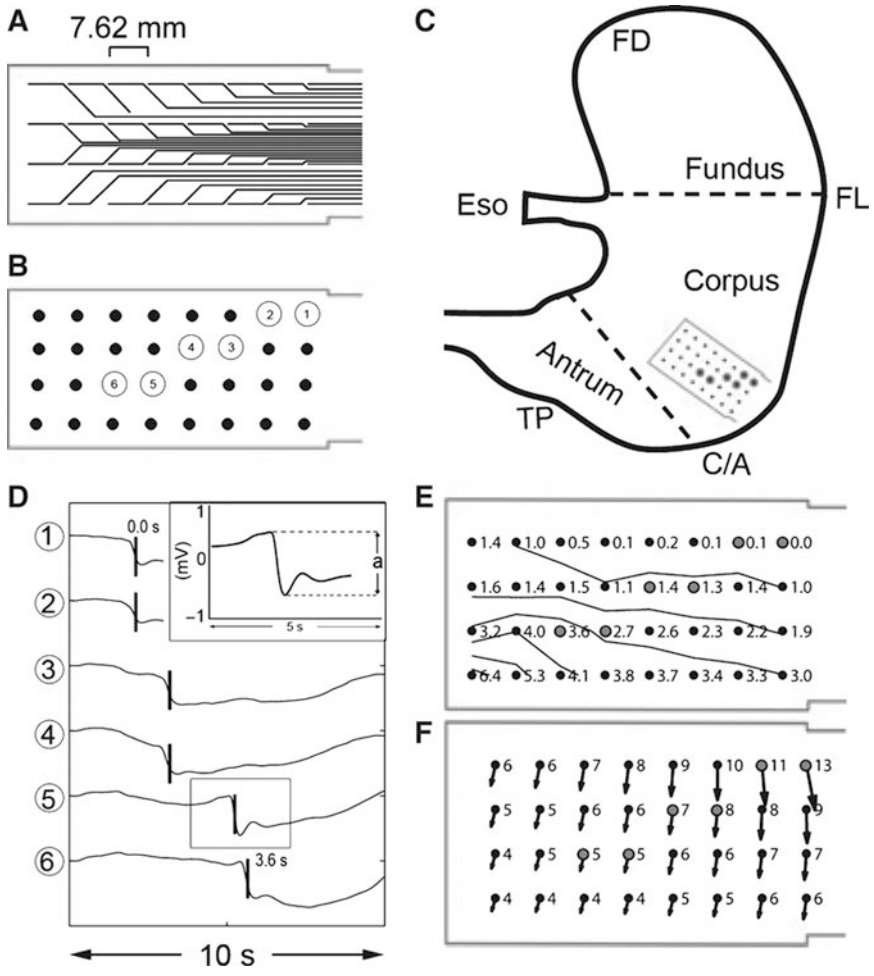

Figure 1.

(A) The flexible Printed Circuit Board (PCB) recording head used in this study (4 × 8 array, interelectrode distance 7.62 mm). (B) Porcine gastric anatomy. FD, fundal diverticulum; Eso, esophagus; TP, torus pyloricus. Two anatomical lines were used to divide the stomach into fundus, corpus, and antrum: (i) FL, fundal line: a horizontal line drawn from the angle of His to the greater curvature; (ii) C/A, corpus–antrum line: a line drawn at a 45° angle from the incisura (a notch on the lesser curvature) to the greater curvature. (C) A dot-matrix representation of the PCB array. (D) An example of slow wave recordings from a PCB electrode (4–6 PCB electrodes were used during this study), placed over the lower corpus (position shown in B), using the configuration shown in C. The inset demonstrates amplitude (a) calculation: the difference between the maximum and the minimum voltage during a slow wave event. (E) The temporal profile of propagating slow wave fronts is graphically represented by activation time mapping. In this example, the isochronal lines demarcate 1 s time intervals. (F) Velocity values at the individual electrode points are represented graphically by velocity arrow plots. The arrow heads are aligned in the direction of the propagating slow wave form, and the arrow lengths are proportional to the slow wave velocity at each electrode point.

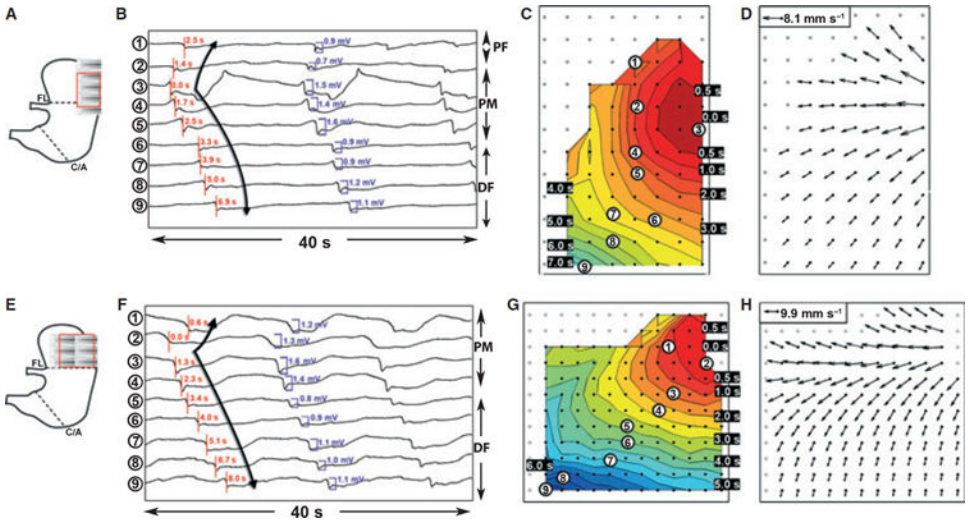

Figure 2.

Examples of slow wave propagation within the pacemaker and fundal regions of two experimental animals. (A, E) Printed Circuit Board (PCB) position diagrams showing the site of the PCB arrays during the recordings; the red rectangles highlight the region represented in the subsequent maps. (B, F) Representative electrograms recorded from the pacemaker region. Activation times from the first cycle are shown in red, and amplitudes from the next cycle are shown in purple. Amplitudes are higher in the vicinity of the gastric pacemaker. (C, G) Activation time maps of the pacemaker region, corresponding to the cycles marked with the arrow in B, F. The isochronal color bands indicate the area of slow wave propagation per 0.5 s intervals. Activity propagates isotropically from the pacemaker site. (D, H) Velocity plots from the same data, demonstrating fast activity in the vicinity of the gastric pacemaker.

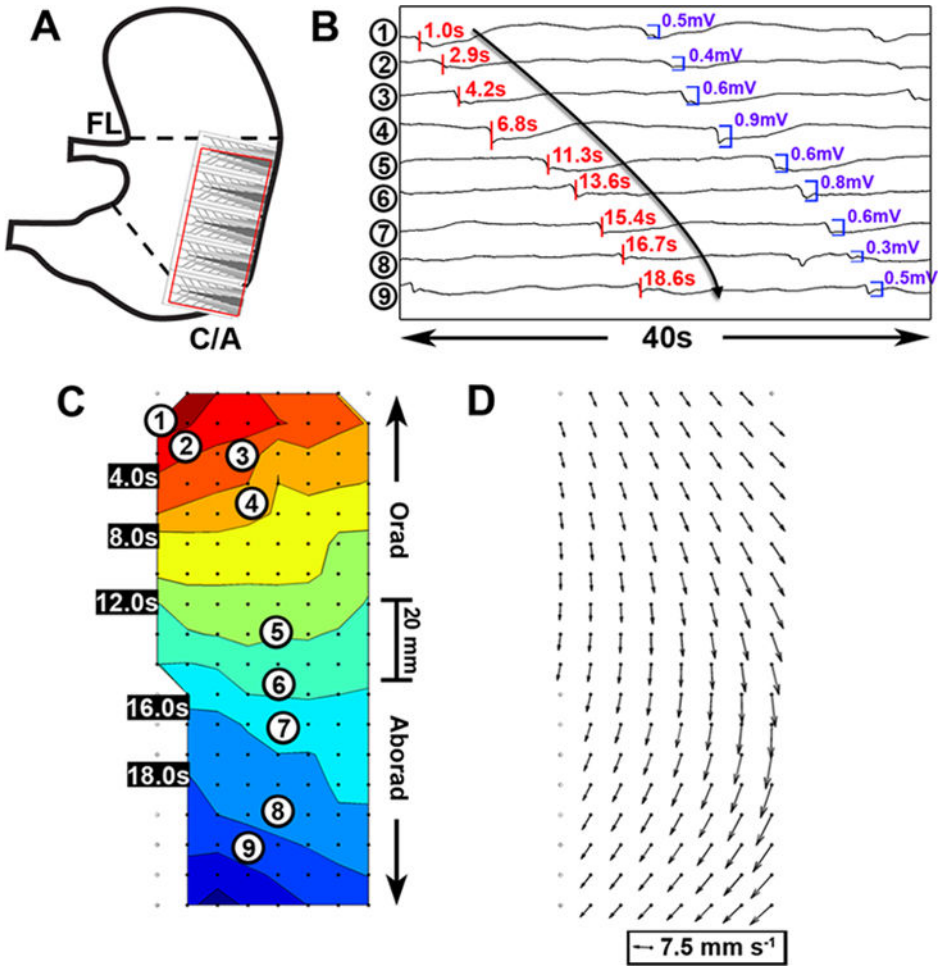

Figure 3.

Slow wave propagation in the corpus and antrum. (A) Printed Circuit Board (PCB) positions for the demonstrated mapped sequence (five PCBs; 160 electrodes total; 77 cm^2). The red outline shows the area of interest in the subsequent maps. (B) Representative electrograms from nine channels, showing consistent slow wave activity through the corpus and antrum. The corpus wavefronts propagate aborally as a circumferential band of activation. (C) Activation time map of the cycle marked by the arrow in (B). The isochronal color bands demonstrate the area of slow wave propagation per 2 s intervals. (D) Velocity plot of the same cycle. There was no difference in wave amplitude or velocity between the proximal corpus, distal corpus, and antrum.

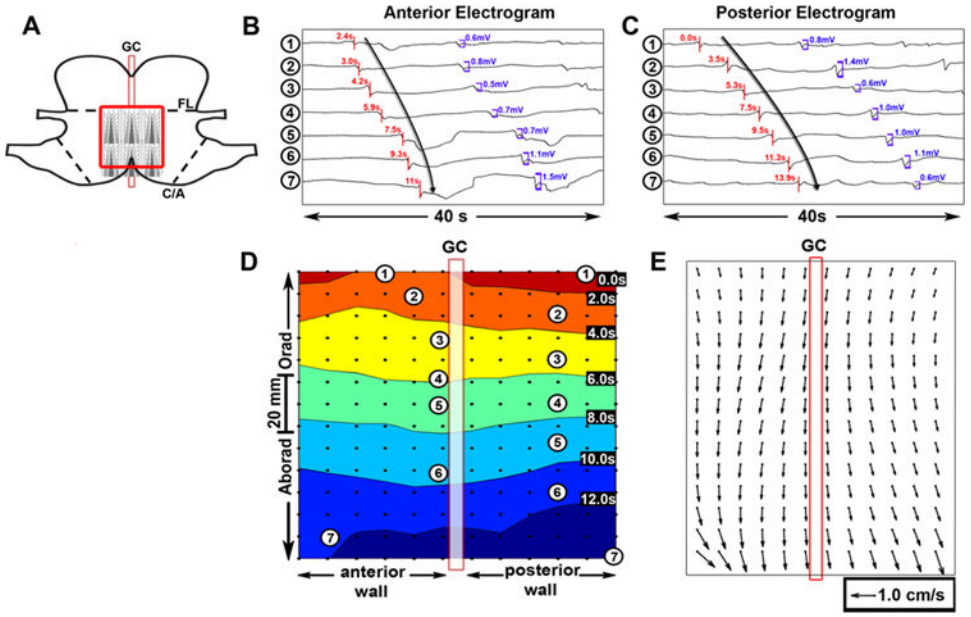

Figure 4.

Simultaneous mapping of the anterior and posterior stomach. (A) Six Printed Circuit Boards (192 electrodes; ~96 cm^2) were wrapped around the greater curvature of the corpus. The red rectangle highlights the region represented in the subsequent maps. (B, C) Representative simultaneous electrogram sequences from the anterior (B) and posterior (C) serosa, showing similar propagation patterns in both regions. (D) Activation time mapping of the sequences designated by arrows in B and C, revealing a circumferential band of activity that propagates down both gastric surfaces in synchrony. (E) The corresponding velocity plot, displaying consistent slow wave velocities across the majority of the mapped field (mean velocity in mapped field = 8.8 mm s^{-1}). GC, greater curvature.

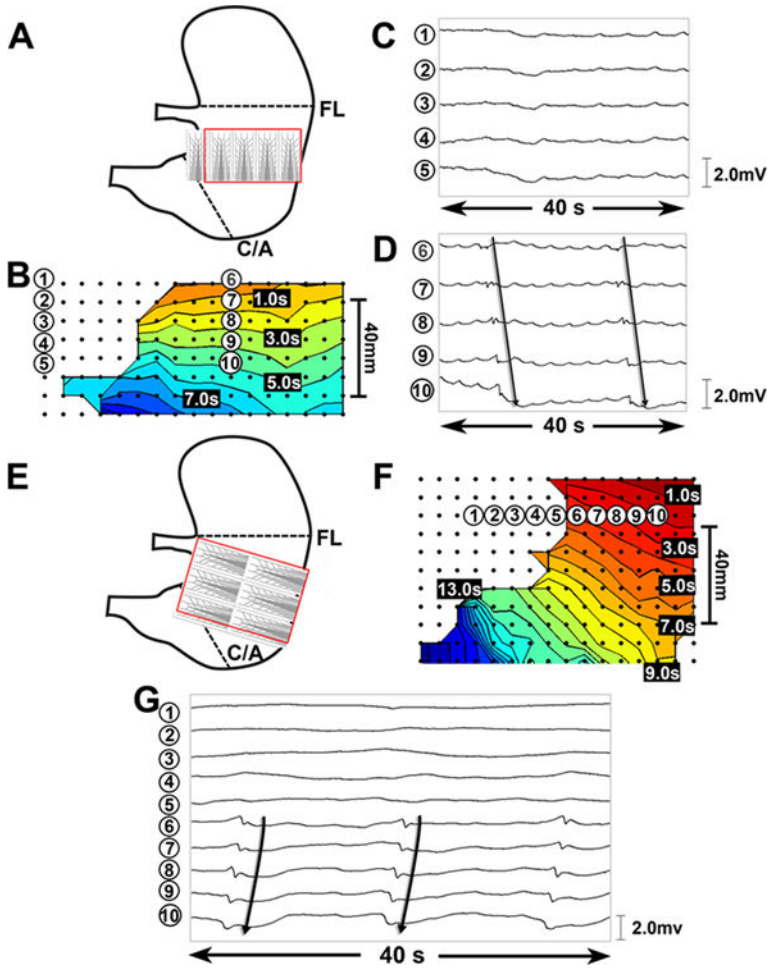

Figure 5.

Examples of electrical quiescence near the lesser curvature, from two experiments. (A, E) Printed Circuit Board (PCB) position diagrams showing the site of the PCB arrays during recording; the red rectangles reflect the regions represented in the subsequent activation maps. (B, F) Activation time (AT) maps of gastric slow waves captured by the PCB arrays. The isochronal color bands indicate the area of slow wave propagation per 1 s intervals. (C, D, G) Representative electrograms recorded from the corpus and antrum from the electrodes indicated on the AT maps. An electrically quiescent region is seen along the left (medial) side of the maps, close to the lesser curvature.

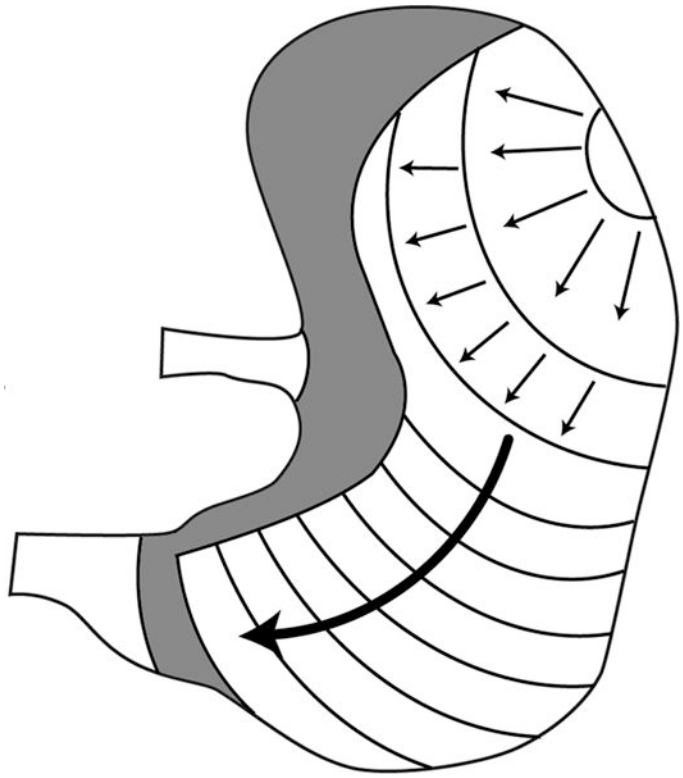

Figure 6.

Summary of porcine gastric slow wave activity. Slow waves originate from a pacemaker site along the greater curvature of the mid fundus. The activity initially propagates radially, but only activates a limited region of the fundus. The shaded areas are electrically quiescent. Propagation is isotropic, rapid and of high-amplitude in the vicinity of the pacemaker region, before dropping by ~30% in velocity and ~30% in amplitude in the adjacent stomach. Propagation continues aborally at a similar amplitude and velocity throughout the corpus and antrum, toward the torus pyloricus, which is electrically quiescent. Slow wave propagation is consistent and continuous across both the anterior and posterior gastric serosal surfaces as shown in Figure 4. Eso, esophagus, TP, torus pyloricus.

Table 1

Regional variations in porcine gastric amplitude and velocity (all values are mean ± SEM).

	*Pacemaker region	Proximal fundus	Distal fundus	Proximal corpus	Distal corpus	Antrum
Amplitudes (mV)	*1.3 ± 0.2	0.8 ± 0.1	0.9 ± 0.1	1.0 ± 0.1	0.9 ± 0.2	1.1 ± 0.2
Velocities (mm s^{-1})	*13.3 ± 1.0	8.1 ± 0.5	9.0 ± 0.6	8.4 ± 0.8	8.3 ± 0.8	6.8 ± 0.6

* $P < 0.05$ *vs* all other gastric regions.